Coinhibition of overexpressed genes in acute myeloid leukemia subtype M2 by gold nanoparticles...

Article *in* Cancer Gene Therapy · August 2016

DOI: 10.1038/cgt.2016.33

CITATION
1

READS
25

14 authors, including:

Behnaz Bazrafshan
Islamic Azad University of Gorgan
9 PUBLICATIONS **3** CITATIONS
SEE PROFILE

Seyedhossein Hekmatimoghaddam
Shahid Sadoughi University of Medical Scien...
103 PUBLICATIONS **240** CITATIONS
SEE PROFILE

Hakim Azizi
Zabol University Of Medical Sciences
5 PUBLICATIONS **12** CITATIONS
SEE PROFILE

Pantea Izadi
3 PUBLICATIONS **6** CITATIONS
SEE PROFILE

Some of the authors of this publication are also working on these related projects:

Review article on protein misfolding View project

Tissue engineering View project

Cancer Gene Therapy (2016) 00, 1–6

www.nature.com/cgt

ORIGINAL ARTICLE

Coinhibition of overexpressed genes in acute myeloid leukemia subtype M2 by gold nanoparticles functionalized with five antisense oligonucleotides and one anti-CD33(+)/CD34(+) aptamer

MA Zaimy[1], A Jebali[2], B Bazrafshan[3], S Mehrtashfar[4], S Shabani[5], A Tavakoli[6], SH Hekmatimoghaddam[2], A Sarli[7], H Azizi[8], P Izadi[1], B Kazemi[9], A Shojaei[10], A Abdalaian[11] and J Tavakkoly-Bazzaz[1,12]

The aim of this study was to evaluate an engineered nanostructure to silence five important oncogenes, including *BAG1*, *MDM2*, *Bcl-2*, *BIRC5* (*survivin*) and *XIAP*, in acute myeloid leukemia subtype 2 (AML-M2). The smart nanostructures were functionalized gold nanoparticles (FGNs) containing five antisense oligonucleotides (AOs) and one anti-CD33(+)/CD34(+) aptamer. First, the best AO for each gene was selected with the OligoWalk online software, and then different arrangements of AOs were evaluated with the RNAstructure software. Thereafter, naked gold nanoparticles (NGNs) were synthesized by the reaction of 1000 mM $HAuCl_4$ with 10 μg ml^{-1} ascorbic acid. Next, five AOs and one anti-CD33(+)/CD34(+) aptamer were attached to NGNs through serial reactions. Later, 5 ml of heparinized blood samples from five AML-M2 patients were prepared, cancerous cells were isolated and then incubated with three concentrations (75, 150 and 300 μg ml^{-1}) each of FGNs, NGNs, gold nanoparticles functionalized with scrambled oligonucleotides (GNFSONs) and doxorubicin. Finally, cell death percentage and gene expressions were measured by MTT (3-(4,5-dimethylthiazol-2-yl)-2,5-diphenyltetrazolium bromide) assay and real-time PCR, respectively. This study showed that FGNs and doxorubicin led to more cell death compared with NGNs and GNFSONs ($P < 0.05$). Interestingly, all concentrations of FGNs led to a decrease in gene expression. As an important finding, although all concentrations of doxorubicin could also inhibit the expression of genes, FGNs had more effect ($P < 0.05$). Moreover, both NGNs and GNFSONs could silence all genes only at a concentration of 300 μg ml^{-1}. For *BCL2* and *XIAP*, a dose-dependent pattern was observed, but there was no similar pattern for others.

Cancer Gene Therapy advance online publication, 12 August 2016; doi:10.1038/cgt.2016.33

INTRODUCTION

Theoretically, acute myeloid leukemia (AML) is associated with some genetic mutations in hematopoietic stem cells.[1] Most of these mutations influence self-renewal, proliferation and differentiation of HSCs.[2] Basically, abnormal or poorly differentiated HSCs are seen in AML patients.[3]

Nowadays, the standard therapy for AML is chemotherapy, that is, in young and old patients, anthracycline and cytarabine are administered, respectively.[4] Moreover, anthracenedione mitoxantrone is used to achieve complete remission.[5,6] It is known that the use of traditional anticancer drugs has some severe side effects.[7–9] Thus, there is an urgent need to develop novel effective therapeutic agents to decrease the unwanted effects. In recent years, some efforts have been made to design targeted therapies for various hematologic malignancies.[10–12] In targeted drug deliveries, malignant cells are targeted by ligands, antibodies or aptamers.[13] Aptamers are either RNA or DNA oligonucleotides or oligopeptides that have unique three-dimensional structures. They can attach to specific molecules—for example, drugs, toxins, proteins, cells and so on. Potentially, they are ideal molecules for targeting malignant cells.[14] Aptamers have some good characteristics—for example, small size, easy purification and low immunogenicity—that make them better than antibodies.[15]

Antisense therapy is a novel method for affecting the expression of important genes. In this method, antisense oligonucleotides (AOs)—for example, small hairpin RNA or small interfering RNA—decrease or silence the expression of target genes.[16,17] To deliver AOs to cells, a suitable carrier is needed. The use of nanoparticles is a good choice.[12] In recent years, some efforts have been made to deliver therapeutic factors into cells

[1]Department of Medical Genetics, School of Medicine, Tehran University of Medical Sciences, Tehran, Iran; [2]Advanced Medical Sciences and Technologies Department, School of Paramedicine, Shahid Sadoughi University of Medical Sciences, Yazd, Iran; [3]Medical Cellular and Molecular Research Center, Golestan University of Medical Sciences, Gorgan, Iran; [4]Department of Biology, Faculty of Basic Sciences, University of Guilan, Rasht, Iran; [5]Department of Biology, Faculty of Science, Zabol University, Zabol, Iran; [6]Department of Molecular Genetics, Science and Research Branch, Islamic Azad University, Zanjan, Iran; [7]Department of Medical Genetics, Faculty of Medical Sciences, Tarbiat Modares University, Tehran, Iran; [8]Department of Medical Parasitology, Zabol University of Medical Sciences, Zabol, Iran; [9]Department of Biotechnology, School of Medicine, Shahid Beheshti University of Medical Sciences, Tehran, Iran; [10]Department of Medical Genetics and Molecular Biology, Faculty of Medicine, Iran University of Medical Sciences, Tehran, Iran and [11]Department of Chemical Engineering, Princeton University, Princeton, NJ, USA. Correspondence: Dr J Tavakkoly-Bazzaz. Department of Medical Genetics and Molecular Biology, Faculty of Medicine, Iran University of Medical Sciences, Tehran, Iran.
E-mail: tavakkolybazzazj@tums.ac.ir or avakkolybazzazj@gmail.com
[12]Current address: Department of Medical Genetics, School of Medicine, Tehran University of Medical Sciences, Tehran, 1417614411, Iran. Tel: 09122108444, Fax: 0098-2188953005
Received 17 May 2016; revised 26 June 2016; accepted 30 June 2016

using nanoparticles.[18] For example, some drugs[19–21] and oligonucleotides[22,23] have been delivered by different nanoparticles, for example, gold nanoparticles, albumin nanoparticles and so on.

The aim of this study was to evaluate an engineered nanostructure to silence five important oncogenes, including *BAG1*, *MDM2*, *Bcl-2*, *BIRC5* (*survivin*) and *XIAP*, in AML subtype 2 (AML-M2). The nanostructure consisted of gold nanoparticles functionalized with five AOs and one anti-CD33(+)/CD34(+) aptamer (functionalized gold nanoparticle (FGN)).

MATERIALS AND METHODS

Materials

Ascorbic acid, $HAuCl_4$, cell culture medium Roswell Park Memorial Institute 1640 (RPMI1640), 3-(4,5-dimethylthiazol-2-yl)-2,5-diphenyltetrazolium bromide (MTT), 1-ethyl-3-(3-dimethylaminopropyl)carbodiimide (EDC), isopropanol, chloroform and Hank's balanced salt solution were purchased from Sigma-Aldrich Chemical (St Louis, MO, USA). All oligonucleotides were sourced from Takapoo Zist Company (Tehran, Iran). RNA extraction buffer (RNX-Plus) and cDNA Synthesis Kits were purchased from Sinaclon Company (Tehran, Iran). The real-time master mix was provided by Applied Biosystems Company (Foster City, CA, USA).

The selection of AOs and their arrangement

At first, five overexpressed genes in AML-M2 were considered, including *BAG1*, *MDM2*, *Bcl-2*, *BIRC5* (*survivin*) and *XIAP*. Then, the common sequence of different mRNA variants of each gene was taken from the NCBI database, using nucleotide blast (nBlast) algorithm. Thereafter, each sequence was submitted to the OligoWalk online software (http://rna.urmc.rochester.edu/servers/oligowalk2/help.html). After that, the best AOs were selected, according to efficacy score. The number of 'U' in AOs was an undesirable factor, and was tried to be maintained as low as possible. In the next step, different arrangements of AOs were built. Moreover, a polyA sequence was placed between each AO sequence. Then, each arrangement was submitted to the RNAstructure software, version 7.5 (University of Rochester Medical Center Mathews lab, Rochester, NY, USA).

Synthesis of gold nanoparticles

Initially, 10 ml of 1000 mM of $HAuCl_4$ was added to 10 ml of 10 μg ml^{-1} ascorbic acid and incubated at room temperature for 30 min. Thereafter, 500 μl of synthesized gold nanoparticles was added to 100 μl of 100 nM polyA-SH (5′-AAAAAAAAAAA-SH) and incubated at room temperature for 30 min to make polyA-modified gold nanoparticles. The mixture was then centrifuged at 3000 r.p.m. for 5 min and washed three times with distilled water.[24]

Functionalization of polyA-modified gold nanoparticle with AOs

At first, 100 μl of polyA-modified gold nanoparticle was added to 100 μl of 150 μg ml^{-1} EDC and 100 μl of 100 nM AO1 (5′-GGGAACGG-NH_2) and incubated at room temperature for 30 min. Thereafter, the mixture was centrifuged at 3000 r.p.m. for 5 min and the supernatant was discarded. In the next step, 100 μl of polyA-modified gold nanoparticle-AO1 was added to 100 μl of 150 μg ml^{-1} EDC and 100 μl of 100 nM polyA-NH_2 (5′-AAAAAA AAAAA-NH_2) and incubated at room temperature for 30 min. The mixture was then centrifuged at 3000 r.p.m. for 5 min and the supernatant was discarded. Other AOs were reacted the same way. In the final step, anti-CD33 (+)/CD34(+) aptamer was added to the structure to make functionalized gold nanoparticles (FGNs). The aptamer had been modified with a 5' 6-carboxyfluorescein (FAM) group. These reactions are illustrated in Figure 1. To characterize FGNs, scanning electron microscopy (Hitachi, Tokyo, Japan) and atomic force microscopy (DME, Herlev, Denmark) were used.

Preparation of cell suspension and treatments

Initially, 5 ml of heparinized blood was taken from five AML-M2 patients and centrifuged at 3000 r.p.m. for 5 min on 4 ml of 2.5% (w v^{-1}) sucrose. Thereafter, the middle layer (cancerous cells) was separated and washed with fresh RPMI1640. In the next step, AML-M2 cells were exposed to three distinct concentrations (75, 150 and 300 μg ml^{-1}) of FGNs, naked gold nanoparticles (NGNs), gold nanoparticles functionalized with scrambled oligonucleotides (GNFSONs) and doxorubicin, and incubated for 3 h at 37 °C. The intervention groups were as follows:

1. AML-M2 cells exposed to 75 μg ml^{-1} FGNs (G. 1).
2. AML-M2 cells exposed to 150 μg ml^{-1} FGNs (G. 2).
3. AML-M2 cells exposed to 300 μg ml^{-1} FGNs (G. 3).
4. AML-M2 cells exposed to 75 μg ml^{-1} NGNs (G. 4).
5. AML-M2 cells exposed to 150 μg ml^{-1} NGNs (G. 5).
6. AML-M2 cells exposed to 300 μg ml^{-1} NGNs (G. 6).
7. AML-M2 cells exposed to 75 μg ml^{-1} GNFSONs (G. 7).
8. AML-M2 cells exposed to 150 μg ml^{-1} GNFSONs (G. 8).
9. AML-M2 cells exposed to 300 μg ml^{-1} GNFSONs (G. 9).
10. AML-M2 cells exposed to 75 μg ml^{-1} doxorubicin (G. 10).
11. AML-M2 cells exposed to 150 μg ml^{-1} doxorubicin (G. 11).
12. AML-M2 cells exposed to 300 μg ml^{-1} doxorubicin (G. 12).
13. AML-M2 cells exposed to phosphate-buffered saline (G.13).

Cell viability measurement by MTT assay

After incubation, 60 μl of 5 μg ml^{-1} MTT was added to 150 μl of treated cells and incubated for 3 h at 37 °C; then, optical densities of wells were read by an enzyme-linked immunosorbent assay reader (Awareness Technologies, Palm City, FL, USA) at 490 nm. Finally, the cell death percentage was calculated for each group.

RNA isolation

RNA isolation was achieved using RNX- Plus buffer. Briefly, 1 ml of cold RNX-Plus was added to 1 ml of treated cells, mixed on vortex for 10 s and incubated for 1 min at room temperature. Thereafter, 200 μl of chloroform was added, shaken for 10 s, incubated for 1 min on ice and then centrifuged at 12 000 r.p.m. for 10 min. Thereafter, its aqueous phase was transferred to a new tube, followed by the addition of an equal volume of 99.9% isopropanol. After mixing and centrifuging at 12000 r.p.m. for 10 min, the supernatant was discarded and 1 ml of 75% ethanol was added to the mixture and centrifuged at 7500 r.p.m. Finally, the supernatant was discarded and the pellet was redissolved in 50 μl of diethylpyrocarbonate (for inactivation of RNases) water before incubation at 60 °C for 10 min. The

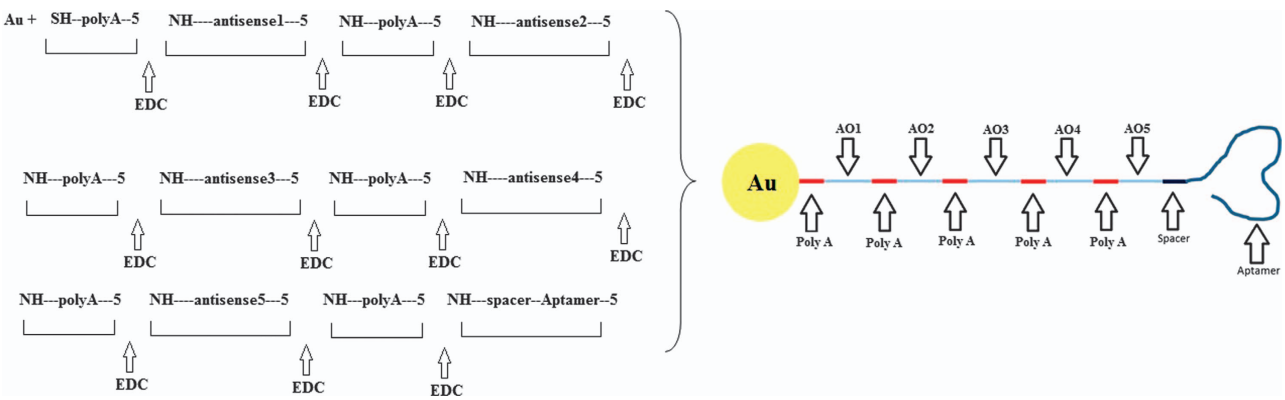

Figure 1. The schematic image of synthesis steps of functionalized gold nanoparticles (FGNs).

Table 1. The details of real-time PCR program

	Cycles				
	1	*45*			*1*
	Step				
	Initial denaturation	*Denaturation*	*Annealing*	*Extension*	*Final extension*
Temperature	95	95	60	72	95
Time (min)	5	1	1	1	5

optical densities of isolated RNA were read at 260 and 280 nm using a NanoDrop products (Wilmington, DE, USA).

cDNA synthesis

Briefly, 1 µg of total RNA and 1 µl of random hexamer were mixed together, and the final volume was adjusted to 10 µl with diethylpyrocarbonate water. Thereafter, the mixture was incubated at 65 °C for 5 min and chilled on ice. Then, 10 µl of RT Premix 2X was added to the mixture, homogenized and incubated at 50 °C for 60 min. The reaction was then stopped by heating at 70 °C for 10 min. Finally, the concentration of synthesized cDNA was read using a Nanodrop.

Real-time PCR

At first, 2 µl of cDNA, 2 µl of forward primer and 2 µl of reverse primer of the interested gene were mixed with 10 µl of SYBR Green Real-Time PCR Master Mix (Applied Biosystems Company) and 4 µl of diethylpyrocarbonate water. Thereafter, all strip tubes were put into a real-time PCR machine (ABI 1 Plus, Foster City, CA, USA) and run according to Table 1. The primers used in this study are all shown in Table 2. Finally, the threshold cycle (C_T) of each gene was read, and its relative expression measured using the following expression ratio formula:

$$\text{Expression ratio} = 2^{-\Delta\Delta C_T} = -[(A-B)-(C-D)]$$

where A is the C_T of the interested gene in the treated group; B the C_T of an internal control gene in the treated group; C the C_T of a target gene in the control group; and D the C_T of an internal control gene in the control group.

Statistical analysis

We ran each test five times, and the results were reported as mean ± s.d. To detect significant differences between groups, one-way analysis of variance was used. For this purpose, the SPSS software (SPSS 20.0 Inc, Chicago, IL, USA) was used, and *P*-values < 0.05 were considered statistically significant.

RESULTS

AO selection and the best arrangement

Table 3 shows the best AO sequence for each gene. As seen, all AOs had high efficacy scores. Table 4 demonstrates different arrangements of AOs and their free energy. Based on this table, ACEBD arrangement was the best, with the least free energy, -0.1 kcal mol^{-1}.

Characterization of FGNs

Figures 2a and b show the scanning electron microscopy and atomic force microscopy images of FGNs, respectively. As is shown, the shape of FGNs was spherical, and its size was < 50 nm.

Cell viability assay

Figure 3 shows the cell death percentage of AML-M2 cells when exposed to FGNs, NGNs, GNFSONs, doxorubicin and phosphate-buffered saline. There was an approximately linear relation between the concentration of FGNs and cell death, that is, an increase in FGN leads to decrease in cell viability. At the same concentration, FGNs led to more cell death than NGNs and GNFSONs ($P < 0.05$). Notably, FGNs and doxorubicin had the same pattern.

Table 2. The sequence of all primers which used in this study

BAG1	Forward	5′-ATGAAGAAGAAAACCCGGCG-3′
	Reverse	5′-CCTGGCTCCGATTCATCTCT-3′
MDM2	Forward	5′-TGCAATACCAACATGTCTGTACCTA-3′
	Reverse	5′-AGGGTCTCTTGTTCCGAAGC-3′
BCL2	Forward	5′-AGATTGATGGGATCGTTGCCT-3′
	Reverse	5′-AGTCTACTTCCTCTGTGATGTTGT-3′
Survivin	Forward	5′-TTTCTCAAGGACCACCGCATC-3′
	Reverse	5′-CAAGTCTGGCTCGTTCTCAG-3′
XIAP	Forward	5′-TGACAAGTGTCCCATGTGCT-3′
	Reverse	5′-CACATCACACATTCAATCAGGGT-3′
GAPDH	Forward	5′-AACTTTGGTATCGTGGAAGGAC-3′
	Reverse	5′-CAGTAGAGGCAGGGATGATG-3′

Table 3. The best AO sequence for each gene

Gene	*Antisense oligonucleotide sequence (5′–3′)*	*Efficacy score*
BAG1	UUGAAGCAGAAGAAACACU	0.99
MDM2	UUACAGCACCAUCAGUAGG	0.99
BCL2	UCAAUCUUCAGCACUCUCC	0.98
Survivin	UUCAAGACAAAACAAGAGC	0.97
XIAP	UAAGAACAACAUAACAUGC	0.97

Abbreviation: AO, antisense oligonucleotide.

Gene expression

Table 5 shows the expression of *BCL2*, *BAG1*, *BIRC5*, *MDM2* and *XIAP* genes in AML-M2 cells exposed to FGNs, NGNs, GNFSONs and doxorubicin. Interestingly, all concentrations of FGN led to decrease in expression of all genes. Although all concentrations of doxorubicin could also inhibit the expression of all genes, FGNs had more effect ($P < 0.05$). It must be mentioned that both NGNs and GNFSONs could only silence genes at concentrations of 300 µg ml^{-1}. For *BCL2* and *XIAP*, a dose-dependent expression pattern was observed, but there was no similar pattern for others.

DISCUSSION

In various cancers, the expression of some genes is changed. Interestingly, gene expression pattern varies from cancer to cancer. In this study, we used antisense technology to target

Table 4. Different arrangements of AOs and their free energy

Free energy (kcal mol^{-1})	*Arrangement*	*Free energy (kcal mol^{-1})*	*Arrangement*	*Free energy (kcal mol^{-1})*	*Arrangement*	*Free energy (kcal mol^{-1})*	*Arrangement*
−0.9	DEABC[a]	−2.8	CDABE	−3.2	BCADE	−1.5	ABCDE
−1	DEACB	−1	CDAEB	−2.2	BCAED	−1.8	ABCED
−0.8	DEBAC	−1.6	CDBAE	−0.7	BCDAE	−1.6	ABDEC
−2.3	DEBCA	−1.4	CDBEA	−0.5	BCDEA	−1.4	ABDCE
−2.7	DECAB	−1.4	CDEAB	−1.9	BCEAD	−2.6	ABEDC
−0.6	DECBA	−1.3	CDEBA	−1	BCEDA	−2.6	ABECD
−1.4	EABCD	−0.9	CEABD	−0.7	BDACE	−0.6	ACBDE
−1.4	EABDC	−2.8	CEADB	−0.7	BDAEC	−1.5	ACBED
−1	EACBD	−2.2	CEBAD	−1.8	BDCAE	−1.4	ACDBE
−1.8	EACDB	−0.8	CEBDA	−0.5	BDCEA	−0.8	ACDEB
−3.4	EADCB	−1.8	CEDBA	−1.3	BDECA	−1.8	ACEDB
−1.3	EBACD	−2.2	DABCE	−0.9	BEACD	−2.8	ADBCE
−2.2	EBADC	−2.6	DABEC	−1.3	BEADC	−2.8	ADBEC
−4.2	EBCAD	−1.3	DACBE	−3.2	BECAD	−2.5	ADCBE
−1.7	EBCDA	−1	DACEB	−0.7	BECDA	−2.2	ADCEB
−1	EBDAC	−1.5	DAEBC	−1.6	BEDAC	−2.9	ADEBC
−2.1	EBDCA	−1.3	DAECB	−2.2	BEDCA	−2.5	ADECB
−2.7	ECABD	−1.5	DBACE	−2.9	CABDE	−1.5	AEBCD
−4.6	ECADB	−1.6	DBAEC	−3.4	CABED	−0.8	AEBDC
−2.5	ECBAD	−2.7	DBCAE	−4.6	CADBE	−0.8	AECBD
−1.1	ECBDA	−1.4	DBCEA	−3.5	CADEB	−1.6	AECDB
−2.1	ECDAB	−1.8	DBEAC	−1.6	CAEBD	−1.8	AEDBC
−1.4	ECDBA	−2.7	DBECA	−3.1	CAEDB	−1.5	AEDCB
−2.5	EDABC	−3.9	DCABE	−2.5	CBADE	−0.6	BACDE
−2.2	EDACB	−2.1	DCAEB	−1.5	CBAED	−1	BACED
−1.9	EDBAC	−1.3	DCBAE	−1.3	CBDAE	−1.9	BADCE
−3.1	EDBCA	−1.1	DCBEA	−0.6	CBDEA	−1.9	BADEC
−3.5	EDCAB	−1.4	DCEAB	−2.5	CBEAD	−0.7	BAECD
−1.5	EDCBA	−0.8	DCEBA	−1.6	CBEDA	−0.9	BAEDC
−2.8	EADBC	−2.5	CEDAB	−0.4	BDEAC	−0.1	ACEBD

Abbreviation: AO, antisense oligonucleotide. [a]A, B, C, D and E represent the AO of *BAG1*, *BCL2*, *Survivin*, *MDM2* and *XIAP*, respectively.

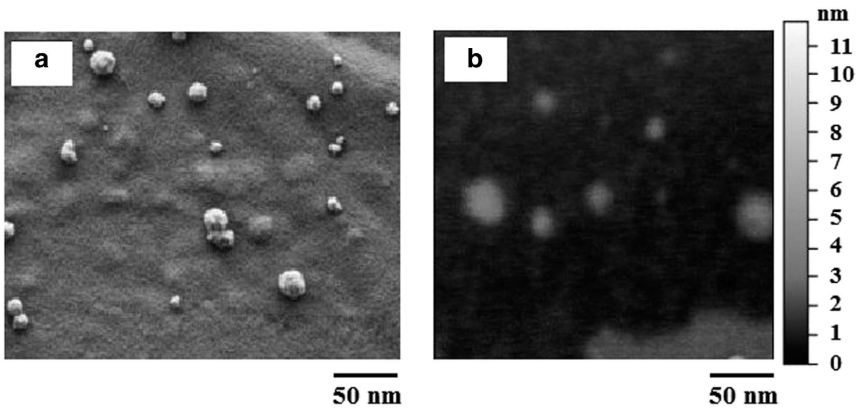

Figure 2. The scanning electron microscopy (SEM) (**a**) and atomic force microscopy (AFM) (**b**) image of functionalized gold nanoparticle (FGNs).

overexpressed genes in AML-M2, as the most common type of AML. AOs identify their targets in mRNA level and easily sit on it. The process is done through the formation of complementary base pairs. It has two outcomes. One is the transformation of single-stranded mRNA to double-stranded mRNA, which can block ribosome binding. Another outcome is degradation of double-stranded mRNA. Generally, RNA-induced silencing complex is activated by the double-stranded mRNA leading to cleavage of the latter. These two outcomes lead to downregulation of the targeted gene.[25–27]

For the first time, we targeted five important genes in AML-M2 cells. For this purpose, a creative antisense structure consisting of five interested antisense sequences and one aptamer was made. In the final structure, a polyA sequence was put between two AOs. In the structure, polyA sequences were sensitive to endonuclease, whereas the antisense parts were resistant. This property had been achieved by replacing phosphate ($P=O$) bonds with sulfate bonds ($S=O$).[28] Because AOs cannot enter cancer cells, it is necessary to provide a carrier to deliver AOs into the cells. In this study, our carrier was gold nanoparticles. These nanoparticles were synthesized with the aid of ascorbic acid, and their size was adjusted to ~50 nm. Then, all AOs were attached to the surface of gold nanoparticles by serial reactions mentioned in the material and methods section. After incubation of FGN and AML-M2 cells, it was observed that FGN could deeply penetrate into AML cells. The penetration of FGN proves that gold nanoparticle are an

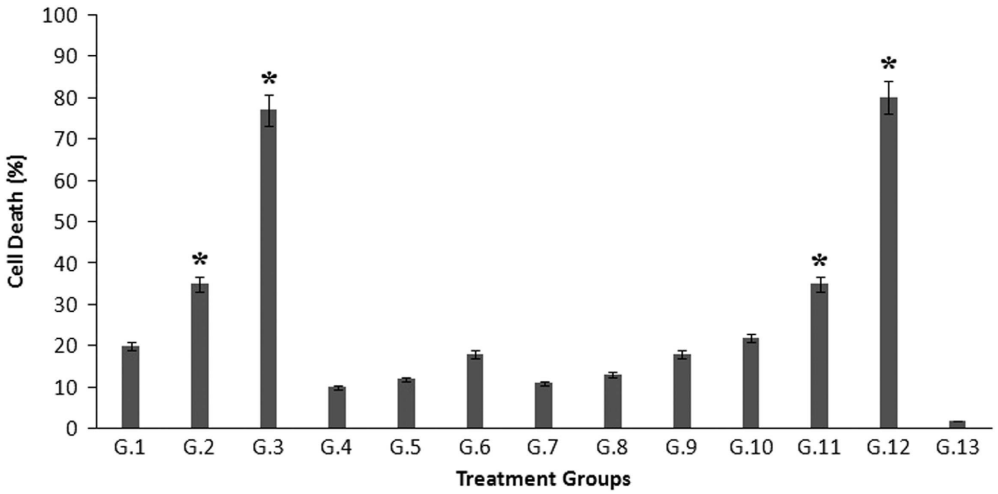

Figure 3. The cell death percentage of acute myeloid leukemia subtype 2 (AML-M2) cells when exposed to functionalized gold nanoparticles (FGNs), naked gold nanoparticles (NGNs), gold nanoparticles functionalized with scrambled oligonucleotides (GNFSONs), doxorubicin and phosphate-buffered saline (PBS). G1 to G13 were described in Materials and methods section. $^*P < 0.05$ compared with other treatment groups, $n = 15$.

Table 5. The expression of *BCL2*, *BAG1*, *BIRC5*, *MDM2* and *XIAP* genes in AML cells when exposed to FGN, NGN, GNFSON and doxorubicin

	BCL2	*BAG*	*Survivin*	*MDM2*	*XIAP*
FGN[a] 75 μg ml^{-1}	0.00007*	0.574	0.101*	0.000009*	0.0004*
FGN 150 μg ml^{-1}	0.07*	0.019*	0.791	0.532	0.07*
FGN 300 μg ml^{-1}	0.319*	0.554	0.259*	0.01*	0.637
NGN[b] 75 μg ml^{-1}	1	1	0.99	1	1
NGN 150 μg ml^{-1}	1	1	1	1	1
NGN 300 μg ml^{-1}	0.9	0.921	0.9	0.963	0.921
GNFSON[c] 75 μg ml^{-1}	0.97	1	1	0.98	1
GNFSON 150 μg ml^{-1}	1	1	0.97	1	1
GNFSON 300 μg ml^{-1}	0.9	0.935	0.9	0.612	0.9
Doxorubicin 75 μg ml^{-1}	0.82	0.85	0.754	0.85	0.89
Doxorubicin 150 μg ml^{-1}	0.84	0.7	0.726	0.82	0.81
Doxorubicin 300 μg ml^{-1}	0.76	0.65	0.725	0.76	0.86

$^*P < 0.05$ compared with others, $n = 15$. Abbreviations: AO, antisense oligonucleotide; FGN, functionalized gold nanoparticle; GNFSON, gold nanoparticles functionalized with scrambled oligonucleotide; NGN, naked gold nanoparticle. [a]Gold nanoparticles functionalized with five AOs and one aptamer. [b]Naked gold nanoparticles. [c]Gold nanoparticles functionalized with scramble oligonucleotides.

appropriate carrier to deliver DNA molecules into cells. It should be noted that we used aptamer molecules as targeting units in FGN. The sequence of the aptamer used in this study was from the study by Zhang *et al*.[29] The aptamer can detect the surface molecules of AML-M2 cells, and facilitate the entrance of FGNs. After ensuring entry of FGNs, MTT assay showed a high degree of cell death, ~70%. This finding confirmed the high toxicity of FGNs, as we expected. Gene expression experiment also showed decrease in targeted mRNAs. Importantly, the rate of gene expression was different for each gene. Here, the critical question is why? The authors think that the delivery rate of FGNs is different for each cell. Moreover, degradation of FGNs is different among various cells. Indeed, the gene-silencing ability was different. At molecular levels, the quantity of gene downregulation was different for each gene. It seems that gold nanoparticles together with AOs have a synergistic effect. The synergism decreases the gene expression and increases the cell death. On the basis of results, it can be stated that gold nanoparticles alone and AOs alone could not decrease gene expression, but FGN could highly affect the expression of all overexpressed genes. The same finding was obtained from MTT assay.

BCL2 is a cell membrane protein involved in blockage of cell apoptosis or programmed cell death. The protein encoded by *BAG1* (BCL2-associated athanogene) binds to *BCL2*, thereby enhancing the antiapoptotic ability of *BCL2*. *MDM2* is an E3 ubiquitin-protein ligase that acts as an oncogene because the encoded protein promotes and accelerates the degradation of tumor suppressors—for example, *p53*, which is the most important tumor suppressor in a cell. *BIRC5* (*survivin*) and *XIAP* are members of the *IAP* apoptotic suppressor protein family. Members of this family have a common domain named baculovirus *IAP* repeat that is necessary for their antiapoptotic properties. They inhibit the apoptotic function of *TRAF1*- and *TRAF2*-encoded proteins. In 2015, Xia *et al*.[30] used small interfering RNA against c-*MYC* in AML cells cocultured with stromal cells. They reported that the treatment significantly induced apoptosis. Mohammadi *et al*.[31] in 2015 used conjugated single-walled carbon nanotubes with aptamer and siNRA against the *BCL9* gene in the breast cancer cell line MCF-7. They found that the use of the structure could induce apoptosis, >20%.[31] In 2006, Bagalkot *et al*.[32] used aptamers as a targeting factor to transfer doxorubicin to prostate cancer cells. They concluded that the use of aptamer is a good way to transfer and target interested materials in cancerous cells.[32] In 2015, Jebali and Anvari-Tafti[22] tried to downregulate *GP63* by AOs conjugated with gold nanoparticles. Their aim was to use the structure for *Leishmania* infections. They reported that the expression of the gene was decreased. Bafghi *et al*.[33] used nanowire conjugated with loop-shaped oligonucleotides to silence cysteine proteinase b gene in *Leishmania tropica*, and showed that the structure could decrease the gene expression.

CONCLUSION

It can be concluded that FGN containing five AOs and one aptamer can affect AML-M2 and lead to cell death. Also, FGN can coinhibit some overexpressed genes including *BCL2*, *BAG1*, *BIRC5*, *MDM2* and *XIAP*. The smart nanostructure may be used to treat

AML-M2, and probably other subtypes, the latter requiring more experiments.

CONFLICT OF INTEREST

The authors declare no conflict of interest.

ACKNOWLEDGEMENTS

This article was extracted from the PhD thesis of Mohammad Ali Zaimy, cosupervised by Dr. J Tavakkoly-Bazzaz and Dr A Jebali. This research was financially supported by the School of Medicine, Tehran University of Medical Sciences, Tehran, Iran (grant number: 31680).

REFERENCES

1 Hope KJ, Jin L, Dick JE. Acute myeloid leukemia originates from a hierarchy of leukemic stem cell classes that differ in self-renewal capacity. *Nat Immunol* 2004; **5**: 738–743.
2 Fröhling S, Scholl C, Gilliland DG, Levine RL. Genetics of myeloid malignancies: pathogenetic and clinical implications. *J Clin Oncol* 2005; **23**: 6285–6295.
3 Gong J, Yu J, Lin H, Zhang X, Yin X, Xiao Z *et al.* The role, mechanism and potentially therapeutic application of microRNA-29 family in acute myeloid leukemia. *Cell Death Differ* 2014; **21**: 100–112.
4 Mancini E, De Martino L, Malova H, De Feo V. Chemical composition and biological activities of the essential oil from *Calamintha nepeta* plants from the wild in southern Italy. *Nat Product Commun* 2013; **8**: 139–142.
5 Moustafa AE-RA, El-Azeem HA, Omran MA, Nasr SA, Nabi IMA, Teleb ZA. Biochemical effect of *Nepeta septemcrenata* growing in South Sinai, Egypt. *Am J Ethnomed* 2015; **2**: 157–168.
6 Tallman MS, Gilliland DG, Rowe JM. Drug therapy for acute myeloid leukemia. *Blood* 2005; **106**: 1154–1163.
7 Tacar O, Sriamornsak P, Dass CR. Doxorubicin: an update on anticancer molecular action, toxicity and novel drug delivery systems. *J Pharm Pharmacol* 2013; **65**: 157–170.
8 Feng S-S. Nanoparticles of biodegradable polymers for new-concept chemotherapy. *Expert Rev Med Dev* 2014; **1**: 115–125.
9 Monsuez J-J, Charniot J-C, Vignat N, Artigou J-Y. Cardiac side-effects of cancer chemotherapy. *Int J Cardiol* 2010; **144**: 3–15.
10 Ju J, Wang N, Wang X, Chen F. A novel all-*trans* retinoic acid derivative inhibits proliferation and induces differentiation of human gastric carcinoma xenografts via up-regulating retinoic acid receptor β. *Am J Transl Res* 2015; **7**: 856.
11 Liu Q, Jin C, Wang Y, Fang X, Zhang X, Chen Z *et al.* Aptamer-conjugated nanomaterials for specific cancer cell recognition and targeted cancer therapy. *NPG Asia Mater* 2014; **6**: e95.
12 Kamaly N, Swami A, Wagner R, Farokhzad OC. *Nanomedicines for Diagnosis and Treatment of Prostate Cancer, Imaging and Focal Therapy of Early Prostate Cancer*. Springer: Berlin, Gemany, 2013, pp 203–217.
13 Estey E, Levine RL, Löwenberg B. Current challenges in clinical development of 'targeted therapies': the case of acute myeloid leukemia. *Blood* 2015; **125**: 2461–2466.
14 Farokhzad OC, Jon S, Khademhosseini A, Tran T-NT, LaVan DA, Langer R. Nanoparticle–aptamer bioconjugates a new approach for targeting prostate cancer cells. *Cancer Res* 2004; **64**: 7668–7672.
15 Vinores S. Technology evaluation: pegaptanib, Eyetech/Pfizer. *Curr Opin Mol Ther* 2003; **5**: 673–679.
16 McManus MT, Sharp PA. Gene silencing in mammals by small interfering RNAs. *Nat Rev Genet* 2002; **3**: 737–747.
17 Dykxhoorn DM, Lieberman J. The silent revolution: RNA interference as basic biology, research tool, and therapeutic. *Annu Rev Med* 2005; **56**: 401–423.
18 Brigger I, Dubernet C, Couvreur P. Nanoparticles in cancer therapy and diagnosis. *Adv Drug Deliv Rev* 2012; **64**: 24–36.
19 Chiannilkulchai N, Driouich Z, Benoit J, Parodi A, Couvreur P. Doxorubicin-loaded nanoparticles: increased efficiency in murine hepatic metastases. *Select Cancer Ther* 1989; **5**: 1–11.
20 Steiniger SC, Kreuter J, Khalansky AS, Skidan IN, Bobruskin AI, Smirnova ZS *et al.* Chemotherapy of glioblastoma in rats using doxorubicin-loaded nanoparticles. *Int J Cancer* 2004; **109**: 759–767.
21 Byeon HJ, Lee S, Min SY, Lee ES, Shin BS, Choi H-G *et al.* Doxorubicin-loaded nanoparticles consisted of cationic- and mannose-modified-albumins for dual-targeting in brain tumors. *J Control Rel* 2016; **225**: 301–313.
22 Jebali A, Anvari-Tafti MH. Hybridization of different antisense oligonucleotides on the surface of gold nanoparticles to silence zinc metalloproteinase gene after uptake by *Leishmania major*. *Colloids Surf B* 2015; **129**: 107–113.
23 Almeida JPM, Figueroa ER, Drezek RA. Gold nanoparticle mediated cancer immunotherapy. *Nanomed Nanotechnol Med* 2014; **10**: 503–514.
24 Khan Z, Singh T, Hussain JI, Hashmi AA. Au (III)–CTAB reduction by ascorbic acid: preparation and characterization of gold nanoparticles. *Colloids Surfaces B* 2013; **104**: 11–17.
25 Ocana A, Perez-Peña J, Serrano-Heras G, Corrales-Sanchez V, Montero J, Gascón-Escribano M *et al.* Abstract P3-14-11: gene-expression analyses identify altered transcription factors and supports the antitumor activity of novel bromodomain inhibitors in triple negative breast cancer. *Cancer Res* 2016; **76**: P3-14-11–P13-14-11.
26 Kole R, Krainer AR, Altman S. RNA therapeutics: beyond RNA interference and antisense oligonucleotides. *Nat Rev Drug Discov* 2012; **11**: 125–140.
27 Wilson RC, Doudna JA. Molecular mechanisms of RNA interference. *Annu Rev Biophys* 2013; **42**: 217–239.
28 Stewart AJ, Canitrot Y, Baracchini E, Dean NM, Deeley RG, Cole SP. Reduction of expression of the multidrug resistance protein (MRP) in human tumor cells by antisense phosphorothioate oligonucleotides. *Biochem Pharmacol* 1996; **51**: 461–469.
29 Zhang S, Wang G, Zhu P, Liang J, Xu Y, Peng M *et al.* [Screening and structure analysis of nucleic acid aptamers binding to surface of CD33 (+)/CD34 (+) cells from patients with acute myeloid leukemia subtype M_2]. *J Exp Hematol Chin Assoc Pathophysiol* 2011; **19**: 561–565.
30 Xia B, Tian C, Guo S, Zhang L, Zhao D, Qu F *et al.* c-Myc plays part in drug resistance mediated by bone marrow stromal cells in acute myeloid leukemia. *Leukemia Res* 2015; **39**: 92–99.
31 Mohammadi M, Salmasi Z, Hashemi M, Mosaffa F, Abnous K, Ramezani M. Single-walled carbon nanotubes functionalized with aptamer and piperazine–polyethylenimine derivative for targeted siRNA delivery into breast cancer cells. *Int J Pharm* 2015; **485**: 50–60.
32 Bagalkot V, Farokhzad OC, Langer R, Jon S. An aptamer–doxorubicin physical conjugate as a novel targeted drug-delivery platform. *Angew Chem Int Ed* 2006; **45**: 8149–8152.
33 Bafghi AF, Jebali A, Daliri K. Silica nanowire conjugated with loop-shaped oligonucleotides: a new structure to silence cysteine proteinase gene in Leishmania tropica. *Colloids Surf B* 2015; **136**: 323–328.